Virology 396 (2010) 135–142

Contents lists available at ScienceDirect

Virology

journal homepage: www.elsevier.com/locate/yviro

Phenylalanines at positions 88 and 159 of *Ebolavirus* envelope glycoprotein differentially impact envelope function

Wu Ou [a,1], Harlan King [a,1,2], Josie Delisle [a], Dashuang Shi [b], Carolyn A. Wilson [a,*]

[a] Division of Cellular and Gene Therapies, Center for Biologics Evaluation and Research, FDA, Bldg. 29B, Room 5NN22, 8800 Rockville Pike, Bethesda, MD 20892, USA
[b] Research Center for Genetic Medicine, Children's National Medical Center, The George Washington University, Washington, D. C. 20010, USA

ARTICLE INFO

Article history:
Received 21 August 2009
Returned to author for revision
16 September 2009
Accepted 16 October 2009
Available online 10 November 2009

Keywords:
Ebolavirus
Envelope glycoprotein
Viral entry
Mutagenesis

ABSTRACT

The envelope glycoprotein (GP) of *Ebolavirus* (EBOV) mediates viral entry into host cells. Through mutagenesis, we and other groups reported that two phenylalanines at positions 88 and 159 of GP are critical for viral entry. However, it remains elusive which steps of viral entry are impaired by F88 or F159 mutations and how. In this study, we further characterized these two phenylalanines through mutagenesis and examined the impact on GP expression, function, and structure. Our data suggest that F159 plays an indirect role in viral entry by maintaining EBOV GP's overall structure. In contrast, we did not detect any evidence for conformational differences in GP with F88 mutations. The data suggest that F88 influences viral entry during a step after cathepsin processing, presumably impacting viral fusion.

Published by Elsevier Inc.

Introduction

Ebolavirus (EBOV) infection causes Ebola hemorrhagic fever with mortality rates up to 90%. The genus *Ebolavirus* belongs to the family Filoviridae and is composed of five species: Zaire, Sudan, Ivory Coast, Bundibugyo, and Reston (Gonzalez et al., 2007; Towner et al., 2008). There are no approved therapies or vaccines, although promising pre-clinical studies have been reported for some *Ebolavirus* vaccines (Reed and Mohamadzadeh, 2007).

EBOV is an enveloped negative strand RNA virus. The envelope glycoprotein (GP) is first synthesized as a precursor (GP0), which is subsequently cleaved by furin into the surface glycoprotein (GP1, aa1–501) and the transmembrane glycoprotein (GP2, aa502–676) (Volchkov et al., 1998). GP1 and GP2 are linked together through a disulfide bond (Jeffers et al., 2002). GP1 contains the receptor binding domain (amino acids 54–201), and GP2 contains the membrane fusion machinery that induces viral and endosomal membrane fusion resulting in release from the endosomes (Chandran et al., 2005; Kuhn et al., 2006; Schornberg et al., 2006; Takada et al., 1997; Volchkov et al., 1998; Wool-Lewis and Bates, 1998). Though the receptor for EBOV remains elusive, several host factors that can aid virus infection have been reported (Alvarez et al., 2002; Chan et al., 2001; Powlesland et al., 2008; Shimojima et al., 2006; Simmons et al., 2003a, 2003b; Takada et al., 2004). Following the binding of GP1 to EBOV receptor, pseudovirions bearing EBOV GP have been shown to undergo endocytosis and GP1 is further processed in endosomes by cathepsin L and/or cathepsin B to generate a fragment of approximately 19 kDa, which remains linked to GP2 through a disulfide bond. Cathepsin processing is currently thought to prime EBOV GP for fusion, which may play a direct or indirect role in exposing the membrane fusion machinery in GP2 (Chandran et al., 2005; Schornberg et al., 2006).

We and others have shown that phenylalanines 88 and 159 in GP1 play important roles in EBOV GP-mediated viral entry (Brindley et al., 2007; Manicassamy et al., 2005; Mpanju et al., 2006). However, it remains unclear which step of viral entry is impaired by mutation of F88 or F159. According to the recently reported GP crystal structure, F88 is partially exposed on the GP1 surface adjacent to the putative receptor binding site and the GP2 internal fusion loop, while F159 is deeply buried within a hydrophobic pocket (Lee et al., 2008) (Fig. 1). Both of these residues are surrounded by a group of hydrophobic amino acids (Fig. 1). The properties of an amino acid are determined by its side chains, including size, shape, charge, polarity, and hydrophobicity. To gain further understanding of how these two phenylalanines affect EBOV GP structure and function, we mutated each phenylalanine to either histidine, valine or tyrosine, and characterized each mutation for its impact on GP's structure and function.

Results

Impact of F88 and F159 mutations on EBOV GP-mediated infection

To gain a better understanding on how F88 and F159 contribute to EBOV GP's structure and function, we further mutated F88 to histidine

* Corresponding author. Fax: +1 301 827 0449.
E-mail address: carolyn.wilson@fda.hhs.gov (C.A. Wilson).
[1] W.O. and H.K. contributed equally to this study.
[2] Current address: Department of Biology Graduate Program, University of Maryland, College Park, MD 20742.

0042-6822/$ – see front matter. Published by Elsevier Inc.
doi:10.1016/j.virol.2009.10.028

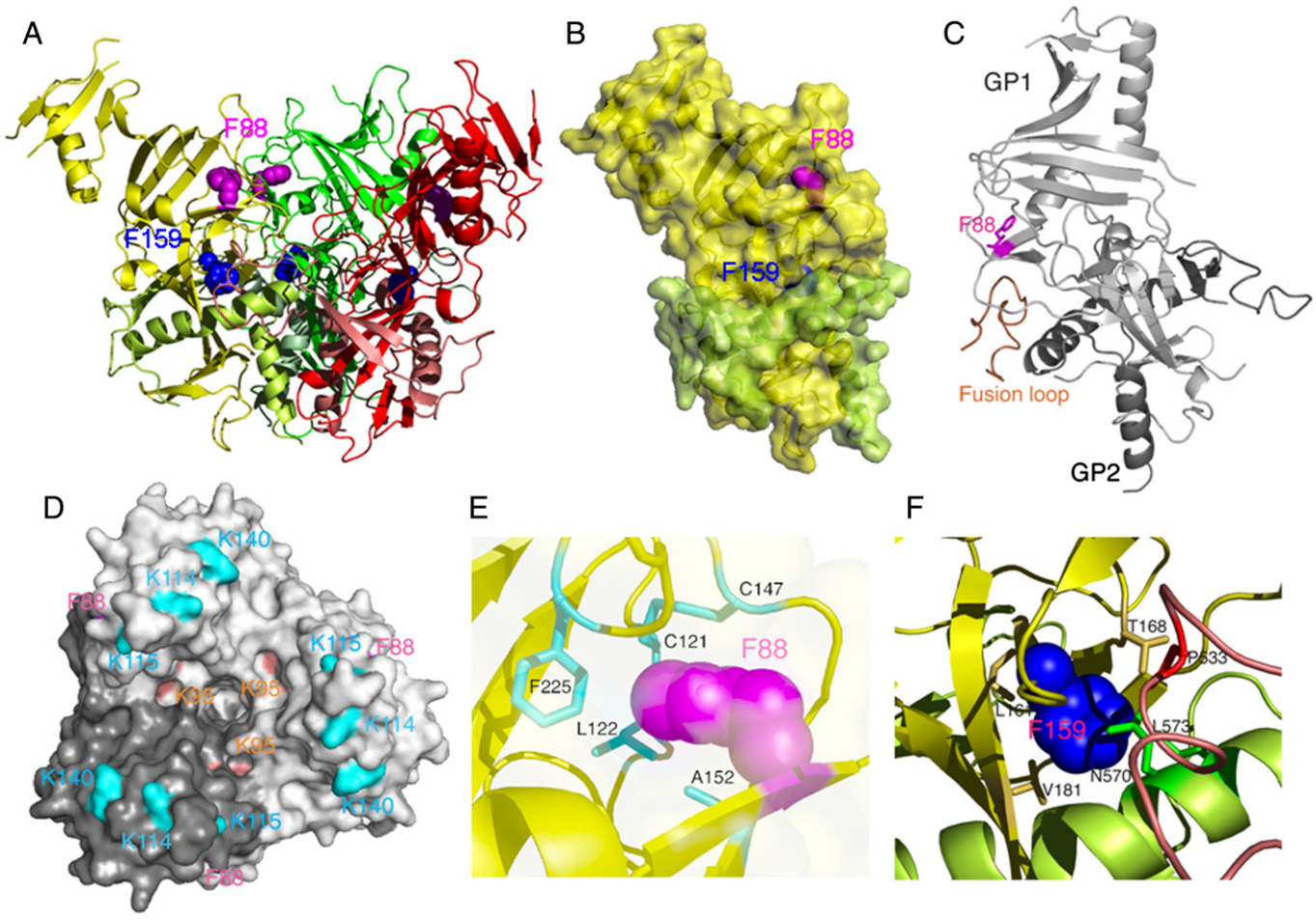

Fig. 1. Crystal structure of EBOV GPΔMucΔTM. (A) Ribbon diagram of EBOV GPΔMucΔTM trimer with one monomer in yellow, another one in green and the third one in red. F88 (purple) and F158 (blue) are highlighted. (B) Filled model structure of a monomer. F88 (purple) is partially exposed while F159 (dark blue) is deeply buried. (C) Ribbon diagram showing the vicinity of F88 to GP2 internal fusion loop (brown). GP1 is shown in light grey, and GP2 in dark grey. (D) Filled model showing the vicinity of F88 to residues that are labeled and suggested to be important for binding to EBOV receptor (based on Dube et al., 2009). (E and F) Ribbon diagrams showing amino acids adjacent to F88 and F159, respectively. Both F88 and F159 are surrounded by a group of hydrophobic amino acids. The graphic structure was produced using Pymol and PDB file 3CSY and is based on the published crystal structure (Lee et al., 2008).

(H), valine (V), or tyrosine (Y), generated MLV(GP) retroviral vector pseudotypes bearing WT or mutant GP, and tested their infectivity on HeLa cells. We found the infectivity titers of F88H, F88V, and F88Y were about 0.3%, 66%, and 93% that of the WT, respectively (Fig. 2). The titer for vectors bearing WT GP was 2230 ± 122 BFU. We also mutated F159 to H, V, or Y, and found the infectivity titers of the MLV (GP) mutants were about 0%, 28%, and 25% of vectors bearing WT GP, respectively (Fig. 2). As we reported previously (Mpanju et al., 2006), retroviral vector pseudotypes carrying GP with F88A or F159A mutations were non-infectious (Fig. 2).

Impact of F88 and F159 mutations on GP expression or incorporation

To determine whether the decrease in infectivity titer was due to a decrease in GP expression or incorporation into the virions, we checked GP expression level in the total lysate, on the cell surface, or on pseudovirions by Western blot. All the mutant GPs were well expressed though their expression level varied slightly (Fig. 3A). The same membrane was stripped and re-blotted with anti-beta actin antibody to confirm that the sample loading was even (Fig. 3B). The cell surface GP level, which should have a direct impact on GP incorporation level on virus particles and hence the titer, did not correlate with the titer, in that cell surface GP was detected even in mutants that had very low or no detectable infectious titer, such as F88H and F159H, suggesting that lack of GP incorporation is not responsible for the poorly infectious phenotype of these mutants (Fig. 3C). Again, the sample loading was confirmed to be even (Fig. 3D). Western blot analysis of the virus-containing crude supernatant also showed comparable levels of GP with only slight variations in GP level that did not correlate with the pseudovirus titer (Fig. 3E).

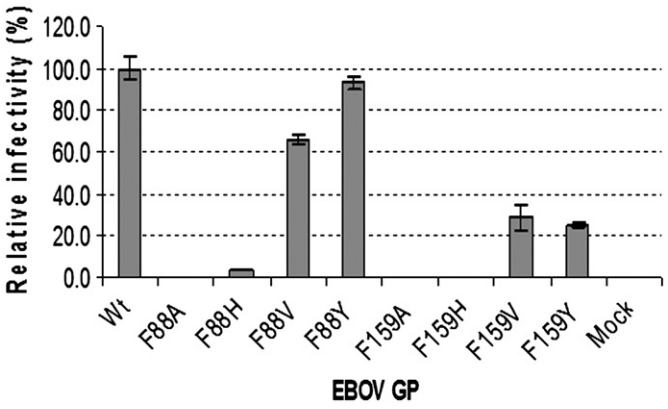

Fig. 2. Infectivity of EBOV GP mutants. HeLa cells were infected with MLV(GP) pseudovirus and histochemically stained for β-galactosidase activity 48 h after infection. Virus titer was determined by counting the blue forming units (BFU) and used to calculate the relative infectivity by normalizing all values to the infectivity titers observed for MLV(WT GP) pseudovirions. The absolute titer for the WT was 2230 ± 122 BFU. In these experiments, mock represents cells exposed to supernatant collected from cells exposed to transfection reagents only in the absence of any DNA.

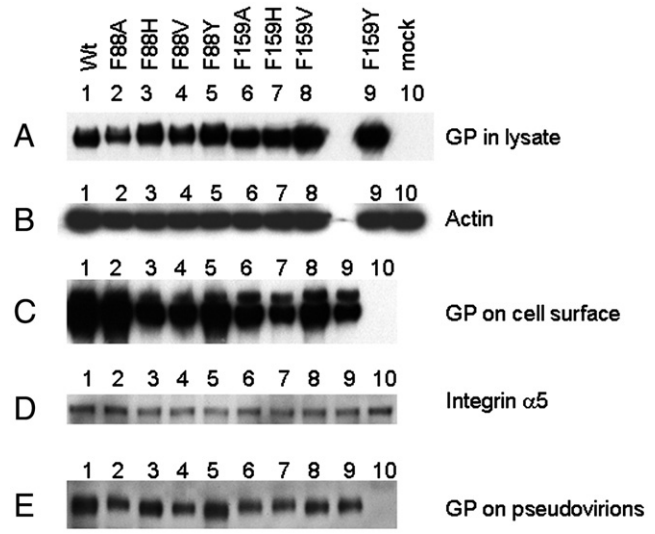

Fig. 3. Western blot detection of EBOV GP. 293T cells were transfected to produce MLV (GP) pseudovirus and lysed 48 h after transfection. (A) Total GP in cell lysate reacted against mouse monoclonal antibody 6D8-1-2. (B) The same membrane used in Fig. 3A was stripped and reacted against a mouse anti-β-actin monoclonal antibody. (C) GP on cell surface detected by antibody 6D8-1-2 following biotinylation of surface proteins using membrane impermeable biotin reagents and purification using streptavidin-coated magnetic beads, as described in Materials and methods. (D) The same membrane used in Fig. 3C was stripped and reacted against a mouse anti-integrin α5 monoclonal antibody. (E) GP in the crude pseudovirus supernatant.

Impact of F88 and F159 mutations on pseudovirus binding to susceptible cells

To determine whether the decrease in infectivity was due to a decrease in binding of retroviral vector pseudotypes to susceptible cells, we evaluated the binding properties of pseudotype vectors carrying the mutant GPs using flow cytometry. Since our assay is different from previously published binding assays for *Ebolavirus* GP (Kaletsky et al., 2007; Kuhn et al., 2006), we first analyzed binding in positive control Vero cells and negative control Jurkat cells. Strong binding of WT GP pseudovirus was detected on susceptible Vero cells, as measured by an approximately 30-fold shift in mean fluorescence intensity (MFI). In contrast, only a very small shift in MFI was detected on Jurkat cells, consistent with previously reported binding assay results (Kaletsky et al., 2007; Kuhn et al., 2006) (Fig. 4A). We then evaluated the binding properties of pseudotype vectors carrying the mutant GPs, and found that F88 mutants bound to Vero cells as efficiently as the WT did, with the only exception of pseudoviruses carrying F88A mutant GP, which showed reduced binding. However, none of the vectors carrying F159 mutant GPs showed a MFI higher than background (Fig. 4B). The same results were observed when the binding assay was repeated at room temperature (data not shown). However, antibody 12B5-1-1, which binds to a linear epitope in the mucin domain (Wilson et al., 2000), was able to detect all mutant GPs on the cell surface, suggesting that the negative binding results for F159 mutants were truly due to lack of virus binding to cells, not due to inability of 12B5-1-1 binding to the mutant GPs (Fig. 5).

Impact of F88 and F159 mutations on GP's overall structure

In spite of comparable or slightly lower levels of GP detected on each of the F159 mutants relative to WT or F88 mutants, no detectable binding was observed for any of the F159 mutants, including those that were infectious. To test whether this was due to mutation-induced overall structure change, we probed the structure of mutant GPs with KZ52, a human monoclonal antibody that recognizes a conformational epitope composed of both GP1 and GP2 (Lee et al., 2008; Maruyama et al., 1999). As a control, we used 12B5-1-1, an antibody that recognizes a linear epitope in the mucin domain and is able to detect all the mutant and WT GPs on the cells from the same transient transfection (Fig. 5). While KZ52 did not detect mutant GPs F159A or F159H, WT GP and other mutant GPs tested were all detectable by KZ52 (Fig. 5). Two

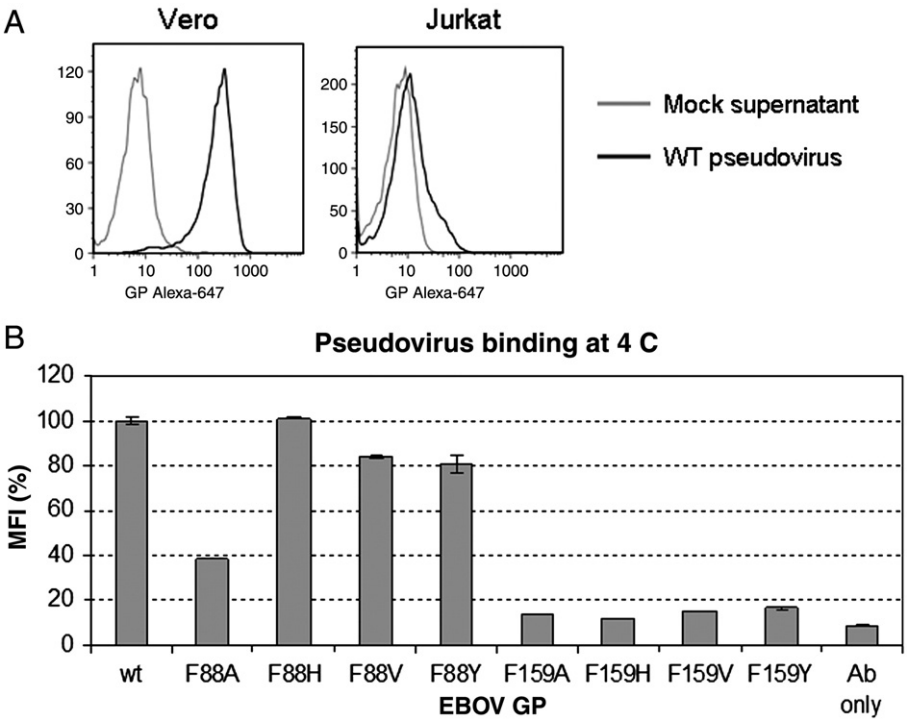

Fig. 4. MLV(GP) pseudovirus binding to cells. (A) Testing of the binding assay. Vero or Jurkat cells were mixed with MLV(WT GP) retroviral vector pseudotype (dark curves) or supernatant of mock-transfected cells (grey curves), stained with mouse anti-EBOV GP monoclonal antibody 12B5-1-1 (linear epitope) at 4 °C, and analyzed on FACSCalibur. Dead cells, which were positive by YO-PRO-1 iodide staining, were excluded for analysis. (B) Binding of pseudovirus carrying WT or mutant GP to Vero cells detected by FACS. Shown was average geometric mean fluorescence intensity +/− StdEv.

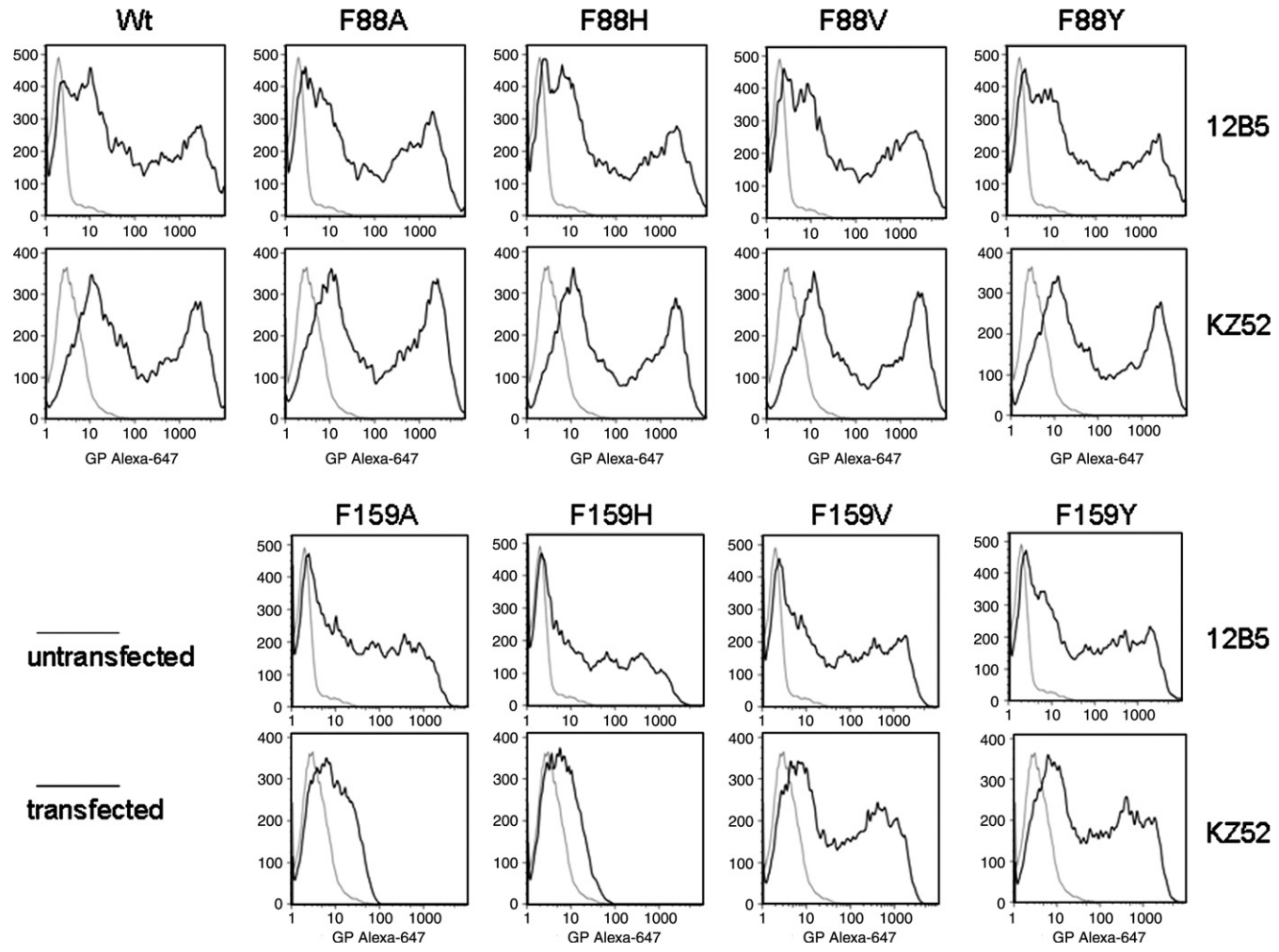

Fig. 5. Monoclonal antibody reactivity with Vero cells transiently expressing WT or mutant GP. COS7 cells were transiently transfected as described in Materials and methods to express WT or mutant GP (dark curves) and then incubated with anti-EBOV GP monoclonal antibodies (KZ52 or 12B5-1-1), Alexa647-anti-mouse/human IgG, and analyzed on FACSCalibur. Dead cells, which were positive by YO-PRO-1 iodide staining, were excluded for analysis. Untransfected control cells (grey curves) were stained and analyzed in the same way.

populations of cells were detected in the transiently transfected samples because the transfection efficiency was not 100%. Additional antibodies that recognize conformational epitopes, 6D3-1-1 and 13C6-1-1, were able to detect all GPs tested, including those not detected by KZ52 (data not shown).

Impact of F88 and F159 mutations on GP processing by thermolysin

Following endocytosis, EBOV GP1 must be proteolytically processed by cathepsins L and B to a fragment of approximately 19 kDa before the membrane fusion machinery in GP2 can be released to induce viral and endosomal membrane fusion (Chandran et al., 2005; Schornberg et al., 2006). In vitro processing of GP by thermolysin, which functions at neutral pH, also generates the same fragment and can be used as a surrogate for cathepsin processing (Dube et al., 2009; Schornberg et al., 2006). To find out whether the structural changes in F159 mutants would alter the thermolysin processing in vitro, we treated retroviral vector pseudotypes with thermolysin and analyzed the processing products by Western blot analysis. The result showed that there was no WT GP left after 10 min of treatment with thermolysin (Figs. 6A and B), the final 19 kDa fragment increased over time while the intermediate product (~44 kDa) decreased (Figs. 6B and C). The same pattern was observed for F88 mutants, but not F159 mutants, which showed no detectable GP at all after thermolysin processing, suggesting the F159 mutants were totally digested by thermolysin (Fig. 6). The weak band of approximately 19 kDa detected for F159 mutants in Figs. 6B and C was background, not GP processing product, because it was detected in the mock control as well.

Discussion

In this study, we characterized the structural and functional impact of the F88 and F159 residues in GP1 by mutating each phenylalanine to histidine, valine, or tyrosine, respectively. As summarized in Table 2, infectivity of retroviral vector pseudotypes carrying the mutant GPs was negatively impacted when the F88 or F159 residues were mutated to alanine (consistent with our prior report) or histidine. The reduced infectivity did not correlate with any change in GP expression or incorporation in viral particles, indicating the mutations impacted viral entry. For F159 mutant GPs, their patterns of binding to Vero cells, reactivity to monoclonal antibodies, and proteolytic digestion by thermolysin were different from those of WT and F88 mutants, suggesting that the F159 residue plays an important role in overall conformation. Substitution of the hydrophobic nonpolar residues at either position 88 or 159 with valine, or isoleucine (Manicassamy et al., 2005) resulted in vectors that were functional, demonstrating that the aromatic side chain of phenylalanine does not appear to be the critical biochemical attribute for viral entry with respect to these two residues.

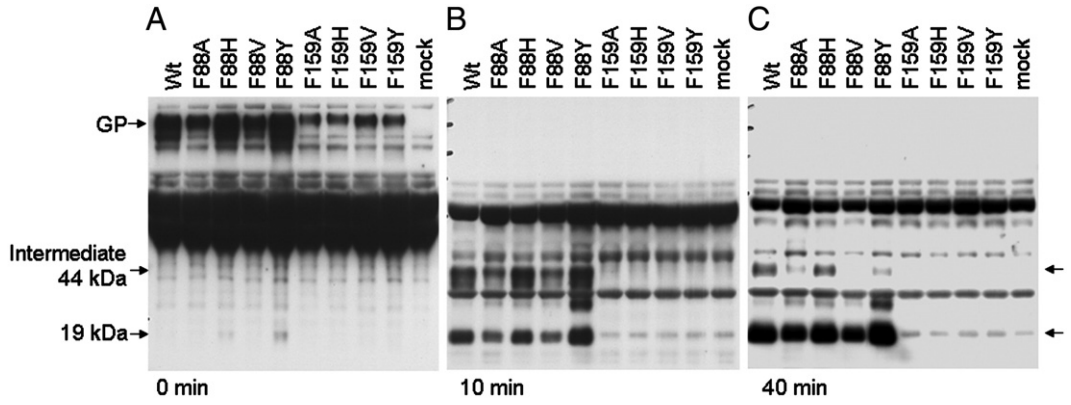

Fig. 6. Proteolytic processing of GP by thermolysin. MLV(GP) pseudovirus supernatant was prepared and then treated with thermolysin for various lengths of time, as described in Materials and methods: 0 min (A), 10 min (B), or 40 min (C). The processed GP product was detected by rabbit anti-EBOV GP peptide polyclonal antibody (R. F88-2) on Western blot. The three membranes were exposed to a same X-ray film, so the exposure time is the same.

No binding activity was detected for F159V and F159Y, although infectivity was detected, but at a somewhat lower titer than for pseudovirus bearing WT GP (Figs. 2 and 4B). Therefore, F159V and F159Y must be able to bind to susceptible cells. The lack of detection of these two mutant GPs' binding to host cells may be a result of a reduced affinity and inability to remain bound during the FACS staining procedures. In contrast, the binding was tight enough to cause infection, suggesting EBOV may not need very tight binding for productive infection to occur.

We performed additional characterization of the impact of the F88 and F159 mutations on overall structure by analyzing the relative reactivity of the mutants to KZ52 antibody that detects a conformational epitope at the interface between GP1 and GP2 (Lee et al., 2008). KZ52 showed similar level of reactivity to the WT or F88 mutant GPs by FACS analysis of transiently transfected cells, including mutants that were non-infectious, F88A and F88H, suggesting that these mutations did not change the conformation of this particular epitope. In contrast, the F159 A and H mutants did not bind to KZ52, indicating the mutation of the F159 residue directly impacted the conformation of the KZ52 epitope. Finally, the sensitivity to proteolytic digestion by thermolysin of F159 mutant GPs was increased. The increased sensitivity for F159 mutants might be due to higher thermolysin to GP ratio (Fig. 6). However, we do not think it is likely because, for example, F88A and F159V quantity was comparable, meaning comparable enzyme to GP ratio, and a strong 19 kDa product band was detected for F88A, while no such product was detected for F159V. The weak 19 kDa bands detected for F159 mutants were background because a band of the same size was detected in the mock control lane. Together, these data indicate that F159 is critical for maintaining GP structure, which determines GP's binding to host cells and proteolytic processing by cathepsin (Table 2). Moreover, the recently published GP crystal structure shows that F159 is deeply buried in a hydrophobic pocket, thus its role in viral entry would have to be through an indirect impact on overall conformation rather than a direct impact on GP binding (Fig. 1).

We demonstrated that both WT and F88 mutant GPs can be partially processed by thermolysin, generating the 19 kDa fragment, consistent with previously reported results of other groups (Chandran et al., 2005; Dube et al., 2009; Schornberg et al., 2006). In previous studies, GP1 in vitro processing by cathepsin or thermolysin was performed on VSV(GP) or FIV(GP) lentiviral vector pseudotypes. We reported for the first time that MLV(WT GP) pseudovirion processing by thermolysin also generated the same 19 kDa fragment, suggesting the structure of EBOV GP on all these different retroviral vector pseudotypes are the same. The conformational change caused by F159 mutations may have altered GP's structure and rendered it more sensitive to thermolysin processing, which could explain why F159 mutants were totally digested/destroyed by thermolysin (Fig. 6). Our results are consistent with an observation made by Brindley et al, who found that F159A mutant is resistant to cathepsin L and is totally digested by cathepsin B (Brindley et al., 2007).

We found that F88 mutants were the same as the WT in most of the examined characteristics, i.e., expression, binding to various antibodies, and sensitivity to thermolysin processing, and the only differences were their infectivity and binding to Vero cells. In our direct binding assay, the binding of F88A to Vero cells was about 32% of that of the wt, suggesting F88 might be important for binding. These observations are similar to Brindley et al. (2007) who showed that a double mutant G87A/F88A inhibited infection of pseudovirions by approximately 55% (Table 2). However, we found that pseudovirions bearing the F88H mutation that are also non-infectious showed binding comparable to WT, indicating that binding may not be the critical role for the F88 residue. Rather, in aggregate, our data for the F88 series of mutations suggests that F88 may impact a step in viral entry after cathepsin processing (Fig. 6, Table 2). While we did not analyze how the F88 mutations impact a post-cathepsin processing step(s), we hypothesize that it may be involved in one of two ways. One hypothesis is that cathepsin processing may further expose F88 and generate a new surface for interacting with an important unknown endosomal factor, and such interaction may be inhibited by F88 mutations (Fig. 1D). A second hypothesis is that F88 mutations may impair the function of the nearby GP2 internal fusion loop (Fig. 1C).

In summary, our study suggests that F159 is a critical amino acid for maintaining EBOV GP's overall structure that is important for proteolytic processing by cathepsin, and thereby the impact on viral infectivity properties is by an indirect mechanism. We also showed that certain mutations of F88 resulted in a loss of infectivity, without any other detectable changes in viral binding (F88H), overall conformation, or thermolysin sensitivity. Therefore, our study suggests that F88 plays an important role in a step after cathepsin processing, not in virus binding. Our study also suggests that weak binding is sufficient for EBOV infection. Together, our findings along with those of others provide important clues for deciphering the detailed entry process of EBOV and for designing antiviral strategies that may block viral infection.

Materials and methods

Cell culture

HeLa, 293T, COS7 and Vero cells were maintained in Dulbecco's Modified Eagle's Medium (DMEM, Lonza, Walkersville, MD) supplemented with 10% fetal bovine serum (FBS, HyClone, Logan, UT), 2 mM

Table 1
Oligonucleotides used for site-directed mutagenesis.

Oligo	Sequence
F88H-F[a]	AACTAAAAGATGGGGCCACAGGTCCGGTGTCCCACCAAAGGT
F88H-R[b]	ACCTTTGGTGGGACACCGGACCTGTGGCCCCATCTTTTAGTT
F88V-F	AACTAAAAGATGGGGCGTCAGATCTGGTGTCCCACCAAAGGT
F88V-R	ACCTTTGGTGGGACACCAGATCTGACGCCCCATCTTTTAGTT
F88Y-F	AACTAAAAGATGGGGCTACAGGTCCGGTGTCCCACCAAAGGT
F88Y-R	ACCTTTGGTGGGACACCGGACCTGTAGCCCCATCTTTTAGTT
F159H-F	TGCCTTCCATAAAGAGGGTGCTCACTTCCTGTATGATCGACTTG
F159H-R	CAAGTCGATCATACAGGAAGTGAGCACCCTCTTTATGGAAGGCA
F159V-F	TGCCTTCCATAAAGAGGGTGCTGTCTTCCTGTATGATCGACTTG
F159V-R	CAAGTCGATCATACAGGAAGACAGCACCCTCTTTATGGAAGGCA
F159Y-F	TGCCTTCCATAAAGAGGGTGCTTACTTCCTGTATGATCGACTTG
F159Y-R	CAAGTCGATCATACAGGAAGTAAGCACCCTCTTTATGGAAGGCA

Note. The underlined sequences encode the mutant amino acids.
[a] F, forward primer.
[b] R, reverse primer.

glutamine, 100 U/mL penicillin, and 100 μg/mL streptomycin (Lonza). Jurkat cells were maintained in RPMI (Lonza) with 10% fetal bovine serum, 2 mM glutamine, 100 U/mL penicillin, and 100 μg/mL streptomycin (Lonza). Cell cultures were grown at 37 °C in a humidified 5% CO_2 incubator.

Antibodies

Mouse anti-EBOV GP monoclonal antibodies 6D3-1-1, 6D8-1-2, 12B5-1-1 and 13C6-1-1 were kindly provided by Dr. Gene Olinger at USAMRIID, Frederick, MD (Wilson et al., 2000). Human anti-EBOV GP monoclonal antibody KZ52 was kindly provided by Dr. Dennis Burton at the Scripps Research Institute, La Jolla, CA (Maruyama et al., 1999). Rabbit polyclonal antibody R.F88-2 was derived by immunizing rabbits four times with a KLH-conjugated peptide of Zaire EBOV GP (aa72–109). The sera were collected two weeks after the last immunization. The peptide was synthesized by NeoMPS (San Diego, CA) and injected by Epitomics (Burlingame, CA). Anti-Rauscher MLV P30 goat antiserum was obtained from ATCC (Manassas, VA). Anti-integrin 5α was from BD Biosciences (San Jose, CA). Anti-β-actin was from Sigma (St. Louis, MO). Horse radish peroxidase (HRP)-conjugated goat anti-mouse IgG and anti-rabbit IgG antibodies were obtained from Pierce (Rockford, IL).

Site-directed mutagenesis

The pVR1012-ZEBOV-GP plasmid that encodes the GP of the WT Zaire EBOV was kindly provided by Dr. Gary Nabel (Vaccine Research Center, NIH, Bethesda, MD) and Dr. Anthony Sanchez (Centers for Disease Control and Prevention, Atlanta, GA). The pVR1012-ZEBOV-GP plasmid was used as the template to generate F88H, F88V, F88Y, F159H, F159V, and F159Y mutants using the QuickChange II XL Site-Directed Mutagenesis Kit (Stratagene, La Jolla, CA) following the manufacturer's instructions. The complimentary oligonucleotides (Table 1) containing the intended mutations were ordered from Integrated DNA Technologies, Inc. (Coralville, IA). The sequence of each mutant was confirmed by the ABI Prism 3100 Sequence Detection System using the BigDye® Terminator v1.1 Cycle Sequencing Kit (Applied Biosystems, Foster City, CA). Mutants F88A and F159A were described previously (Mpanju et al., 2006).

Generation of retroviral vector pseudotypes

To generate retroviral vector pseudotypes bearing Zaire EBOV GP (MLV(GP)), 293T cells were seeded in 100 mm cell culture dishes at a density of 5×10^6 cells/dish and transfected 24 h later with 60 μL Lipofectamine 2000 /dish (Invitrogen, Carlsbad, CA) and three plasmids: 7 μg pVR1012-ZEBOV-GP (WT or mutant), 3.5 μg pMLV-GagPol, and 14 μg of pRT43.2Tnlsβgal that encodes a Moloney murine leukemia virus (MoMuLV)-based packageable genome containing the packaging signal and sequences encoding β-galactosidase with a nuclear localization signal (Finer et al., 1994). Forty-eight hours after transfection, the culture supernatant, which contains the retroviral vector pseudotypes, was filtered through 0.45 μm filter (Millipore), aliquoted, and frozen on dry ice and then transferred to a −80 °C freezer for storage until needed. The cell lysate was harvested for Western blot (as described below). The resulting pseudotypes are composed of a MLV core surrounded by

Table 2
Summary of phenotypes of EBOV GP mutants.

Mutation	Present study								
	wt	F88				F159			
		A	H	V	Y	A	H	V	Y
Infectivity (%)	100	0	0.3	66	93	0	0	28	25
GP in virions[a]	+	+	+	+	+	+	+	+	+
Binding to Vero (%)[b]	100	32	101	83	79	5	4	7	8
Binding to KZ52[b]	+	+	+	+	+	−	−	+	+
Binding to 12B5-1-1[b]	+	+	+	+	+	+	+	+	+
19 kDa product[c]	+	+	+	+	+	−	−	−	−
Effects on GP functions[d]	N/A	III	III	III	III	I, II, IV	I, II, IV	I, II	I, II

Mutation	Brindley et al.			Manicassamy et al.			
	F88[e]	F159		F88			F159
	A	A	L	A	I	E	A
Infectivity (%)	0	0	100	1	104	0	1
GP in virions[a]	+	+	N/A	+	+	+/−	+
Infection competition(%)	45	39.8	N/A	N/A	N/A	N/A	N/A
19 kDa Product Product[f]	+	−	N/A	N/A	N/A	N/A	N/A
Effects on GP function[d]	I	IV	N/A	N/A	None	IV	IV

N/A: not analyzed or not applicable.
[a] Detected by Western blot.
[b] Detected by FACS.
[c] Processed by thermolysin.
[d] I, binding; II, cathepsin processing; III, post cathepsin processing; IV, conformation or protein expression/incorporation into virion.
[e] Analyzed as part of a double mutant, F88A and G87A.
[f] Processed by cathepsin B and L.

EBOV GP on the surface and a retroviral genome encoding the lacZ reporter gene (Table 2).

Viral infectivity assay

One day prior to infection, HeLa cells were seeded in 12-well cell culture plates at a density of 70,000 cells/well. On the day of infection, the culture medium was removed and replaced with 1 mL of vector-containing supernatant that was supplemented with 8 μg/ml polybrene (American Bioanalytical, Natick, MA). Forty-eight hours after exposure to vector-containing supernatant, cells were washed twice with PBS, fixed, and histochemically stained for β-galactosidase activity. Virus titer was determined by counting the blue forming units (BFU) as determined by microscopic examination, as previously described (Wilson and Eiden, 1991).

Western blot analysis

Western blot analysis was performed for both cell lysate and cell surface proteins. To prepare the cell lysate, 293T cells that were transfected to generate retroviral vector pseudotypes as described above were washed once with PBS, detached by gently striking the dishes, transferred to 5 ml tubes, centrifuged for 5 min at 400×*g*. Pelleted material was frozen on dry ice, thawed and lysed for 30 min on regular ice in lysis buffer: RIPA buffer (150 mM NaCl, 1% (v/v) Triton X-100, 0.5% (w/v) NaDOC, 0.1% (w/v) SDS, 50 mM Tris pH 8.0) supplemented with the Complete Mini protease inhibitor cocktail (1 tablet/7 mL, Roche Applied Science, Indianapolis, IN). The lysate was cleared by centrifugation for 10 min at 13,000 rpm at 4 °C in a bench top microcentrifuge. To prepare cell surface proteins, a second set of 293T cells that were transfected in the same way as described above were washed once with PBS, resuspended in PBS supplemented with 1 mg/mL membrane impermeable EZ-Link Sulfo-NHS-LC-LC-Biotin (Pierce), and incubated for 1 h on ice to biotinylate cell surface proteins. After biotinylation, the cells were washed once with PBS supplemented with 100 mM glycine (Sigma) to quench the excess biotin reagent, washed one more time with plain PBS, and lysed using the same lysis buffer and conditions as described above. Streptavidin-coated magnetic beads (MyOne Streptavidin T1, Invitrogen) were mixed on a bench-top rotator with pre-cleared lysate from the biotinylated cells for 1 h at room temperature to capture the biotinylated cell surface proteins. To wash the beads, the supernatant was removed while the beads were captured by Dynal MPC-S magnet (Invitrogen), then the beads were resuspended in 1 ml cold RIPA buffer and rotated for 5 min at room temperature. In total, four washes were performed. The biotinylated proteins were eluted by boiling the beads in 1× NuPAGE LDS Sample Buffer (Invitrogen) for 5 min, resolved on a pre-cast NuPAGE 4–12% Bis-Tris Gel (Invitrogen), and transferred to PVDF membrane (Invitrogen) to do Western blot analysis. The membrane was blotted with one of the following primary antibodies: 6D8-1-2 diluted at 1:10,000, anti-integrin α5 at 1:5000, anti-actin at 1:5000, or anti-P30 at 1:10,000, then blotted with horse radish peroxidase (HRP)-conjugated secondary antibodies diluted at 1:10,000, and finally developed using the Western Lightning™ Plus Chemiluminescence Reagent (PerkinElmer, Waltham, MA) following the manufacture's instructions.

Virus binding assay

Vero cells in T75 flasks (BD, Franklin Lakes, NJ) at a density of 80% confluency were washed twice with PBS, detached in PBS supplemented with 5 mM EDTA, and incubated with 3 mL vector-containing supernatant for 90 min on a rotator at 4 °C to allow the virus to bind to the cells (10^6cells/sample). Then the cells were washed once with 3 mL FACS Wash Buffer (PBS supplemented with 2.5% FBS and 2.5 mM EDTA), then stained for 90 min at 4 °C with the primary antibody 12B5-1-1 diluted at 1:100 in 200 μL FACS Staining Buffer: Invitrogen's CO_2-Independent Medium supplemented with 2.5% FBS and 2.5 mM EDTA. Following one wash with the FACS Wash Buffer, the cells were stained for 60 min at 4 °C with Alexa647-conjugated anti-mouse IgG (Invitrogen) diluted at 1:100 in 200 μL FACS Staining Buffer, washed twice with 3 mL FACS Wash Buffer, resuspended in 500 μL FACS Wash Buffer supplemented with 0.1 μL cell viability dye YO-PRO-1 iodide (Invitrogen), and immediately analyzed by FACSCalibur (BD Biosciences). Jurkat cells were cultured in suspension, stained and analyzed in the same manner as for Vero cells.

Flow cytometry analysis

COS7 cells were seeded in 100 mm cell culture dishes at a density of 3×10^6 cells/dish and transfected 24 h later with 12 μg pVR1012-ZEBOV-GP or mutated derivatives described above, and 30 μL Lipofectamine 2000 per dish. Thirty-six hours after transfection, the cells were washed twice with PBS, detached in PBS supplemented with 5 mM EDTA, and incubated for 90 min at 4 °C with one of the following primary antibodies: 6D3-1-1, 12B5-1-1, 13C6-1-1 (1:100) or KZ52 (1:200) diluted in 200 μL FACS Staining Buffer. Following one wash with 3 mL FACS Wash Buffer, the cells were incubated for 60 min at 4 °C with Alexa647-conjugated anti-mouse IgG (Invitrogen) (for cells incubated with 6D3-1-1, 12B5-1-1, 13C6-1-1) or Alexa647-conjugated anti-human IgG (Invitrogen) (for cells incubated with KZ52) diluted at 1:100 in 200 μL FACS Staining Buffer, washed twice with 3 mL FACS Wash Buffer, resuspended in 500 μL FACS Wash Buffer supplemented with 0.1 μL cell viability dye YO-PRO-1 iodide (Invitrogen), and immediately analyzed by FACSCalibur. Dead cells were excluded by YO-PRO-1 iodide staining. FlowJo (Tree Star, Ashland, OR) was used to analyze the data.

Thermolysin processing

Eight-tenths of one milliliter of retroviral vector pseudotype-containing supernatant was mixed with 15 mL HM reaction buffer (20 mM HEPES (4-(2-hydroxyethyl)-1-piperazineethanesulfonic acid), 20 mM MES (2-(N-morpholino) ethanesulfonic acid), 130 mM NaCl, pH 7.5), then centrifuged through 100 kDa Amicon filters (Millipore, Billerica, MA) for 15 min at 3000×*g*, and 300 μL virus in HM buffer was recovered. Thermolysin (Sigma) was prepared by dissolving the powder in HM buffer that was supplemented with 0.2 mM $CaCl_2$ to a final concentration of 0.5 mg/mL. The buffer-exchanged supernatants were mixed with equal volume of thermolysin and incubated at 37 °C for 0, 10 or 40 min. The reaction was stopped by adding 4× NuPAGE LDS Sample Buffer (Invitrogen) to a final concentration of 1× and boiled for 5 min at 99 °C. The processed and un-processed GP on retroviral vector pseudotypes were resolved on NuPAGE 4–12% Bis-Tris Gels (Invitrogen) and detected by Western blot using R.F88-2 (1:10,000) as the primary antibody, HRP-conjugated anti-rabbit IgG (1:10,000) as the secondary antibody, and Western Lightning™ Plus Chemiluminescence Reagent (PerkinElmer) as the substrate.

Acknowledgments

Plasmids pVR1012-ZEBOV-GP was kindly provided by Dr. Gary Nabel (Vaccine Research Center, NIH, Bethesda, MD) and Dr. Anthony Sanchez (CDC, Atlanta, GA). Mouse monoclonal antibodies against EBOV GP were kindly provided by Dr. Gene Olinger at the USAMRIID. The authors thank Mr. Evan Ewers and Ms. Seton Pariser for technical assistance. No official support or endorsement of this article by the Food and Drug Administration or the Centers for Disease Control and Prevention is intended or should be inferred.

References

Alvarez, C.P., Lasala, F., Carrillo, J., Muniz, O., Corbi, A.L., Delgado, R., 2002. C-type lectins DC-SIGN and L-SIGN mediate cellular entry by Ebola virus in cis and in trans. J. Virol. 76 (13), 6841–6844.

Brindley, M.A., Hughes, L., Ruiz, A., McCray Jr., P.B., Sanchez, A., Sanders, D.A., Maury, W., 2007. Ebola virus glycoprotein 1: identification of residues important for binding and postbinding events. J. Virol. 81 (14), 7702–7709.

Chan, S.Y., Empig, C.J., Welte, F.J., Speck, R.F., Schmaljohn, A., Kreisberg, J.F., Goldsmith, M.A., 2001. Folate receptor-alpha is a cofactor for cellular entry by Marburg and Ebola viruses. Cell 106 (1), 117–126.

Chandran, K., Sullivan, N.J., Felbor, U., Whelan, S.P., Cunningham, J.M., 2005. Endosomal proteolysis of the Ebola virus glycoprotein is necessary for infection. Science 308 (5728), 1643–1645.

Dube, D., Brecher, M.B., Delos, S.E., Rose, S.C., Park, E.W., Schornberg, K.L., Kuhn, J.H., White, J.M., 2009. The primed Ebolavirus glycoprotein (19-kilodalton GP1,2): sequence and residues critical for host cell binding. J. Virol. 83 (7), 2883–2891.

Finer, M.H., Dull, T.J., Qin, L., Farson, D., Roberts, M.R., 1994. kat: a high-efficiency retroviral transduction system for primary human T lymphocytes. Blood 83 (1), 43–50.

Gonzalez, J.P., Pourrut, X., Leroy, E., 2007. Ebolavirus and other filoviruses. Curr. Top. Microbiol. Immunol. 315, 363–387.

Jeffers, S.A., Sanders, D.A., Sanchez, A., 2002. Covalent modifications of the Ebola virus glycoprotein. J. Virol. 76 (24), 12463–12472.

Kaletsky, R.L., Simmons, G., Bates, P., 2007. Proteolysis of the Ebola virus glycoproteins enhances virus binding and infectivity. J. Virol. 81 (24), 13378–13384.

Kuhn, J.H., Radoshitzky, S.R., Guth, A.C., Warfield, K.L., Li, W., Vincent, M.J., Towner, J.S., Nichol, S.T., Bavari, S., Choe, H., Aman, M.J., Farzan, M., 2006. Conserved receptor-binding domains of Lake Victoria marburgvirus and Zaire ebolavirus bind a common receptor. J. Biol. Chem. 281 (23), 15951–15958.

Lee, J.E., Fusco, M.L., Hessell, A.J., Oswald, W.B., Burton, D.R., Saphire, E.O., 2008. Structure of the Ebola virus glycoprotein bound to an antibody from a human survivor. Nature 454 (7201), 177–182.

Manicassamy, B., Wang, J., Jiang, H., Rong, L., 2005. Comprehensive analysis of Ebola virus GP1 in viral entry. J. Virol. 79 (8), 4793–4805.

Maruyama, T., Rodriguez, L.L., Jahrling, P.B., Sanchez, A., Khan, A.S., Nichol, S.T., Peters, C.J., Parren, P.W., Burton, D.R., 1999. Ebola virus can be effectively neutralized by antibody produced in natural human infection. J. Virol. 73 (7), 6024–6030.

Mpanju, O.M., Towner, J.S., Dover, J.E., Nichol, S.T., Wilson, C.A., 2006. Identification of two amino acid residues on Ebola virus glycoprotein 1 critical for cell entry. Virus Res. 121 (2), 205–214.

Powlesland, A.S., Fisch, T., Taylor, M.E., Smith, D.F., Tissot, B., Dell, A., Pohlmann, S., Drickamer, K., 2008. A novel mechanism for LSECtin binding to Ebola virus surface glycoprotein through truncated glycans. J. Biol. Chem. 283 (1), 593–602.

Reed, D.S., Mohamadzadeh, M., 2007. Status and challenges of filovirus vaccines. Vaccine 25 (11), 1923–1934.

Schornberg, K., Matsuyama, S., Kabsch, K., Delos, S., Bouton, A., White, J., 2006. Role of endosomal cathepsins in entry mediated by the Ebola virus glycoprotein. J. Virol. 80 (8), 4174–4178.

Shimojima, M., Takada, A., Ebihara, H., Neumann, G., Fujioka, K., Irimura, T., Jones, S., Feldmann, H., Kawaoka, Y., 2006. Tyro3 family-mediated cell entry of Ebola and Marburg viruses. J. Virol. 80 (20), 10109–10116.

Simmons, G., Reeves, J.D., Grogan, C.C., Vandenberghe, L.H., Baribaud, F., Whitbeck, J.C., Burke, E., Buchmeier, M.J., Soilleux, E.J., Riley, J.L., Doms, R.W., Bates, P., Pohlmann, S., 2003a. DC-SIGN and DC-SIGNR bind Ebola glycoproteins and enhance infection of macrophages and endothelial cells. Virology 305 (1), 115–123.

Simmons, G., Rennekamp, A.J., Chai, N., Vandenberghe, L.H., Riley, J.L., Bates, P., 2003b. Folate receptor alpha and caveolae are not required for Ebola virus glycoprotein-mediated viral infection. J. Virol. 77 (24), 13433–13438.

Takada, A., Robison, C., Goto, H., Sanchez, A., Murti, K.G., Whitt, M.A., Kawaoka, Y., 1997. A system for functional analysis of Ebola virus glycoprotein. Proc. Natl. Acad. Sci. U. S. A. 94 (26), 14764–14769.

Takada, A., Fujioka, K., Tsuiji, M., Morikawa, A., Higashi, N., Ebihara, H., Kobasa, D., Feldmann, H., Irimura, T., Kawaoka, Y., 2004. Human macrophage C-type lectin specific for galactose and N-acetylgalactosamine promotes filovirus entry. J. Virol. 78 (6), 2943–2947.

Towner, J.S., Sealy, T.K., Khristova, M.L., Albarino, C.G., Conlan, S., Reeder, S.A., Quan, P.L., Lipkin, W.I., Downing, R., Tappero, J.W., Okware, S., Lutwama, J., Bakamutumaho, B., Kayiwa, J., Comer, J.A., Rollin, P.E., Ksiazek, T.G., Nichol, S.T., 2008. Newly discovered Ebola virus associated with hemorrhagic fever outbreak in Uganda. PLoS Pathog. 4 (11), e1000212.

Volchkov, V.E., Feldmann, H., Volchkova, V.A., Klenk, H.D., 1998. Processing of the Ebola virus glycoprotein by the proprotein convertase furin. Proc. Natl. Acad. Sci. U. S. A. 95 (10), 5762–5767.

Wilson, C.A., Eiden, M.V., 1991. Viral and cellular factors governing hamster cell infection by murine and gibbon ape leukemia viruses. J. Virol. 65 (11), 5975–5982.

Wilson, J.A., Hevey, M., Bakken, R., Guest, S., Bray, M., Schmaljohn, A.L., Hart, M.K., 2000. Epitopes involved in antibody-mediated protection from Ebola virus. Science 287 (5458), 1664–1666.

Wool-Lewis, R.J., Bates, P., 1998. Characterization of Ebola virus entry by using pseudotyped viruses: identification of receptor-deficient cell lines. J. Virol. 72 (4), 3155–3160.